

Weak lasing in one-dimensional polariton superlattices

Long Zhang^{a,1}, Wei Xie^{a,1}, Jian Wang^a, Alexander Poddubny^{b,c}, Jian Lu^a, Yinglei Wang^a, Jie Gu^a, Wenhui Liu^a, Dan Xu^a, Xuechu Shen^a, Yuri G. Rubo (Юрий Рубо)^{d,2}, Boris L. Altshuler^{e,2}, Alexey V. Kavokin^{f,g}, and Zhanghai Chen^{a,2}

^aState Key Laboratory of Surface Physics, Key Laboratory of Micro and Nano Photonic Structure (Ministry of Education), Department of Physics, Collaborative Innovation Center of Advanced Microstructures, Fudan University, Shanghai 200433, China; ^bTheory of Quantum Coherent Phenomena in Solids, Centre of Nanoheterostructure Physics, Ioffe Physical Technical Institute of the Russian Academy of Sciences, St. Petersburg 194021, Russia; ^cThe Metamaterials Laboratory, Information Technologies, Mechanics, and Optics University, St. Petersburg 199034, Russia; ^dCoordinación de Física Teórica, Instituto de Energías Renovables, Universidad Nacional Autónoma de México, Temixco, Morelos 62580, Mexico; ^ePhysics Department, Columbia University, New York, NY 10027; ^fSpin Optics Laboratory, St. Petersburg State University, St. Petersburg 198504, Russia; and ^gPhysics and Astronomy School, University of Southampton, Highfield, Southampton, SO171BJ, United Kingdom

Contributed by Boris L. Altshuler, February 11, 2015 (sent for review November 20, 2014; reviewed by Chih-Wei Lai and Mikhail Portnoi)

Bosons with finite lifetime exhibit condensation and lasing when their influx exceeds the lasing threshold determined by the dissipative losses. In general, different one-particle states decay differently, and the bosons are usually assumed to condense in the state with the longest lifetime. Interaction between the bosons partially neglected by such an assumption can smear the lasing threshold into a threshold domain—a stable lasing many-body state exists within certain intervals of the bosonic influxes. This recently described weak lasing regime is formed by the spontaneously symmetry breaking and phase-locking self-organization of bosonic modes, which results in an essentially many-body state with a stable balance between gains and losses. Here we report, to our knowledge, the first observation of the weak lasing phase in a one-dimensional condensate of exciton–polaritons subject to a periodic potential. Real and reciprocal space photoluminescence images demonstrate that the spatial period of the condensate is twice as large as the period of the underlying periodic potential. These experiments are realized at room temperature in a ZnO microwire deposited on a silicon grating. The period doubling takes place at a critical pumping power, whereas at a lower power polariton emission images have the same periodicity as the grating.

weak lasing | superlattice | polariton | condensate | symmetry breaking

The application of artificial periodic potentials to electrons and photons causes a rich variety of phenomena, from electronic minibands in semiconductor superlattices to characteristic stop bands in photonic crystals (1–4). These phenomena form the basis for further developments of optoelectronics. Cavity polaritons (5, 6) (quasi-particles formed by the strong coupling of confined photons with excitons) attracted much attention in recent years due to the remarkable coherent effects linked to their half-matter, half-light nature (7–11). As a result, a new area of physics at the boundary between solid-state physics and photonics has emerged.

Experiments on spatially inhomogeneous polariton condensation are usually interpreted assuming that all one-particle states have the same lifetime (12, 13). Lifting off this assumption leads to the prediction (14) of the “weak lasing” state of interacting polaritons: a type of condensate stabilized by the spontaneous reduction of the symmetry rather than by the dissipation nonlinearities due to, e.g., reservoir depletion. In this work we report, to our knowledge, the first experimental observation of room-temperature polariton condensation in 1D superlattices, which brings clear evidence for the weak lasing state.

The polariton superlattice was assembled using a ZnO microrod with a hexagonal cross-section: a natural whispering gallery resonator to efficiently confine exciton–polaritons (15, 16). Setting the microrod on a silicon slice with periodically arranged channels (Fig. 1) allowed us to avoid the intrinsic structural diffraction typical for the structures with periodic patterns deposited on top of microcavities (17).

The polaritons in this structure were created by nonresonant continuous wave (or long pulse) optical pumping at room temperature, and they were characterized by angle-resolved and spatially resolved photoluminescence (ARPL and SRPL) from the top of the microcavity. The periodic potential caused by the silicon grating manifested itself by a characteristic folded dispersion of the lower polariton branch, revealed in the ARPL images (Fig. 2). One can see the avoided crossing of the polariton dispersion branches resulting in a distinct band gap near the Bragg plane. At strong enough pumping the polariton condensation demonstrates a striking feature: the condensate is formed at the excited polariton states near the energy gaps (states *A*, Fig. 3*A*) rather than at the ground state: the π -state condensate (17).

We checked the spatial coherence of condensates at state *A* by interferometry experiments. Fig. 3*E* and *F* shows two SRPL images of the condensates coming from the two arms of the Michelson interferometer; Fig. 3*F* shows the inversion of the pattern Fig. 3*E* by a retroreflector. Fig. 3*G* shows the interference pattern created by the superposition of the two images with the relative time delay smaller than the coherence time of the polariton condensate (~ 3 ps). The arrows indicate unambiguous interference fringes between two condensates separated by 6 μm . The interference patterns can be observed even for a separation as large as 10 μm , i.e., the π -state condensate

Significance

Bose–Einstein condensation of polaritons in periodically modulated cavities is a very interesting fundamental effect of the physics of many-body systems. It is also promising for application in solid-state lighting and information communication technologies. By a simple microassembling method, we created periodically modulated polariton condensates at room temperature, and observed the stabilization of the coherent condensate due to the spontaneous symmetry-breaking transition. This manifests a previously unidentified type of phase transition, leading to a novel state of matter: the weak lasing state. The optical imaging in both direct and reciprocal space provides clear evidence for the weak lasing in the specific range of the pumping intensities.

Author contributions: Y.G.R., B.L.A., A.V.K., and Z.C. designed research; L.Z., W.X., J.W., J.L., Y.W., J.G., W.L., D.X., X.S., Y.G.R., B.L.A., A.V.K., and Z.C. performed research; L.Z., W.X., J.W., A.P., J.L., Y.W., J.G., W.L., D.X., X.S., Y.G.R., B.L.A., A.V.K., and Z.C. analyzed data; and L.Z., W.X., A.P., Y.G.R., B.L.A., A.V.K., and Z.C. wrote the paper.

Reviewers: C.-W.L., Michigan State University; and M.P., University of Exeter.

The authors declare no conflict of interest.

¹L.Z. and W.X. contributed equally to this work.

²To whom correspondence may be addressed. Email: zhanghai@fudan.edu.cn, ygr@ieir.unam.mx, or bla@physics.columbia.edu.

This article contains supporting information online at www.pnas.org/lookup/suppl/doi:10.1073/pnas.1502666112/-DCSupplemental.

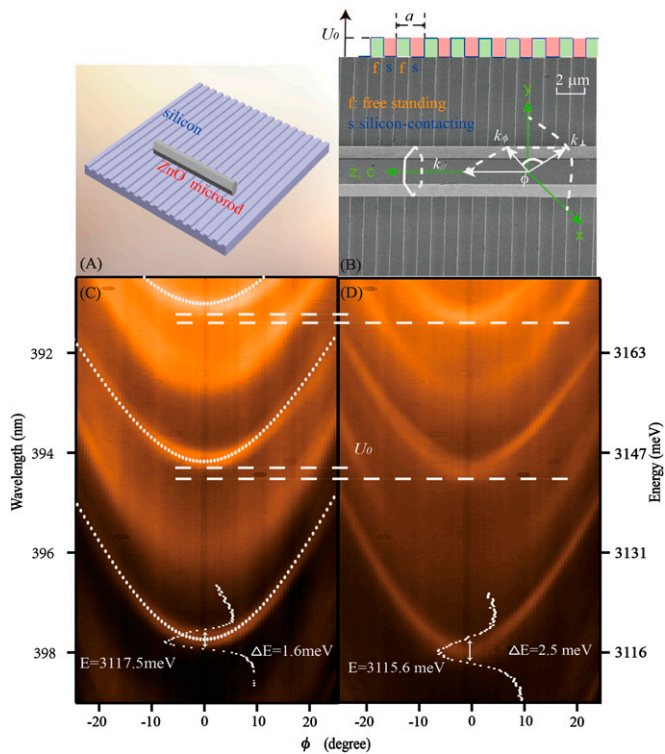


Fig. 1. Illustration of the assembled polaritonic superlattice based on a ZnO–Si microstructure. (A) Schematic representation of the 1D polaritonic crystal. (B) Scanning electron microscope image (top view) of a ZnO microwire with hexagonal cross-section placed on a periodic Si grating. The 1- μm -wide silicon channels equally spaced with the internal distance $a = 2 \mu\text{m}$ apply a static periodic potential to the polaritons with amplitude $ReU \sim 2 \text{ meV}$. The “s” and “f” mark the silicon-contacting parts and the freestanding parts of the microcavity, respectively. (C and D) ARPL spectral images taken under continuous He–Cd laser (325-nm) excitation. TE (electric field component of light along the z axis) polariton modes are shown. (C) Emission from a freestanding ZnO microwire. The white dashed curves are theoretical fits of the lower polariton branches. (D) The same ZnO microwire lying on a flat silicon surface. The peak position and the lineshape at $k_{\parallel} = 0$ are identified. The horizontal dashed lines indicate the lower polariton energy shift (ReU). The incidence angle ϕ is linked with the in-plane wave vector of light by $k_{\parallel} = (E/\hbar c)\sin \phi$, where E is the photon energy.

(17) in our superlattices indeed demonstrates a long-range coherence.

Besides creating the potential wells for polaritons, the contacts of the ZnO microwire with the patterned Si substrate affect the polariton dissipation: In the contact regions (inside the wells) the losses are stronger. This effect naturally explains the π -state condensation: as it is shown in Fig. 3C the minima of the probability amplitude of the state A are at the contact regions, i.e., the polaritons in this state live longer than in the other state A' at the edge of the Brillouin zone, which has maxima at the contact regions. The ground state D with zero wave vector k is distributed between the wells and the barriers more equally and thus possesses an intermediate lifetime. The presence of long-living states at the Bragg gap edges has been previously observed in experiments on X-ray diffraction in crystals (18) and referred to as the Borrmann effect. A similar effect is known to suppress light localization in disordered photonic crystals (19). We calculated the lifetime of polariton states for the different folded dispersion branches in the simplified Kronig–Penney model (see *SI Text* for details) and found that in the A state the polaritons indeed live longer than in the

states A' and D , as shown in Fig. 3B (red color corresponds to the longer lifetime): $\tau_A > \tau_D > \tau_{A'}$.

It is safe to assume that all polariton states within the Brillouin zone have approximately the same influx rate W , which is proportional to the external pumping rate P . Accordingly, as W increases, the lasing condition $W\tau \geq 1$ is satisfied for the A state first. Given the period of the structure a , the emission from this state contains plane waves with wave vectors $k_{\parallel} = \pm\pi(2n+1)/a$, where $n = 0, \pm 1, \pm 2, \dots$.

However, the condensate in the A state becomes unstable for interacting polaritons at the second threshold $W_2 > W_1 = \tau_A^{-1}$ (see *SI Text* for details). The condensed state for $W > W_2$ is stabilized by the gradually increasing admixture of the D state to the A state. The experimental values of pumping that correspond to the first and the second threshold are $P_1 \approx 10 \text{ nW}$ and $P_2 \approx 20 \text{ nW}$. The admixture of the D state is the manifestation of the weak lasing regime (14) characterized by a spontaneous symmetry breaking. Indeed, the condensate wave function can be written as

$$\Psi(z) = C_A \psi_A(z) + C_D \psi_D(z), \quad [1]$$

where $\psi_{A,D}$ are the single-polariton wave functions of the A and D states, and the polariton density $|\Psi(z)|^2$ in this state is not periodic with the period a of the underlying lattice. Instead, it is periodic with the period $2a$: because the signs of $\psi_A(z)$ are opposite in the neighboring barriers, while the signs of $\psi_D(z)$ are the same, the amplitudes of $|\Psi(z)|$ are different in odd and even barriers. As we show in *SI Text*, the weak lasing condensate can be formed in two equivalent states, with coefficients $C_{A,D}$ having the same signs in one state and opposite signs in the other. In both cases, the condensate acquires the double period $2a$, and in addition to the pure A -state emission pattern there appears an emission line at $k_{\parallel} = 0$ (with possible weak satellites at $k_{\parallel} = \pm 2\pi n/a$).

We observed the period doubling of the polariton condensate in both ARPL and SRPL images (Fig. 4). At low pumping, the emission has the same periodicity in real space as the superlattice, whereas for pumping above the second threshold of about 20 nW the emission pattern doubles its period. We have checked that for $P > 20 \text{ nW}$ the three peaks at $k_{\parallel} = 0, \pm\pi/a$ in Fig. 4C indeed correspond to the same frequency and are mutually coherent. At large pumping, the ratio of the intensity of the $k_{\parallel} = 0$ peak to the intensity of the $k_{\parallel} = \pm\pi/a$ peaks saturates at about 0.6,

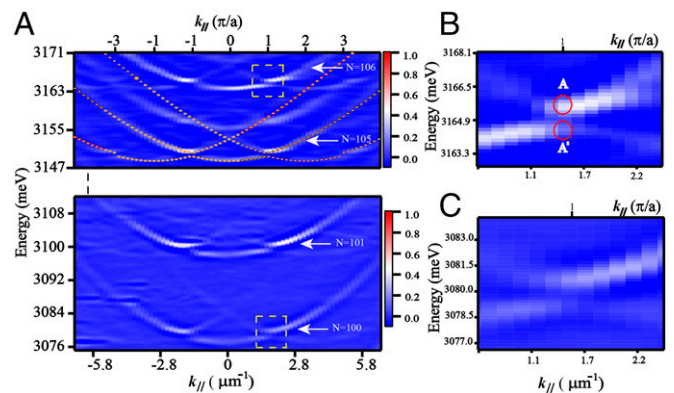


Fig. 2. Dispersion of exciton–polaritons in momentum space demonstrating formation of a polariton superlattice. (A) Photoluminescence mapping (second derivative) in k space under continuous excitation at room temperature. White dashed curves display the calculated dispersion with a band gap ($\Delta E = 0.7 \text{ meV}$). (B and C) Enlarged regions identified by the dashed rectangles in A, respectively, exhibiting the anticrossing dispersion and well-resolved energy gap.

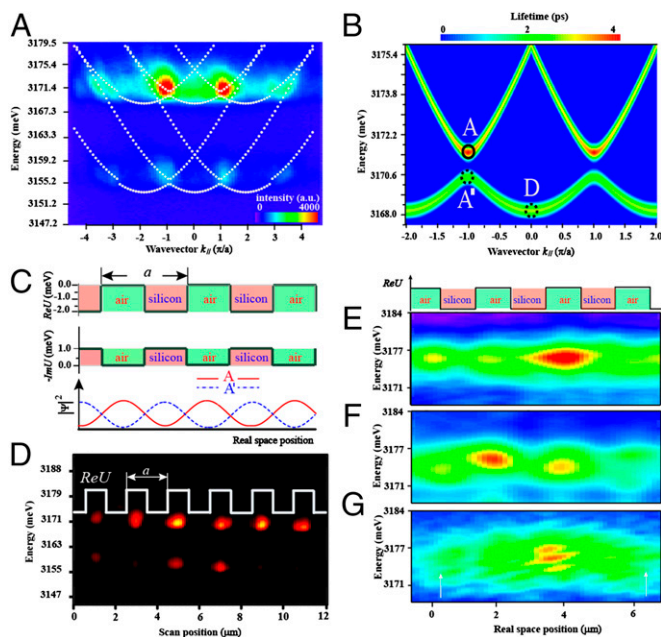


Fig. 3. Polariton condensation at the π -states. (A) Polariton lasing at the edges of the mini-Brillouin zone in k space at room temperature. White dashed curves display the calculated dispersion with a band gap $\Delta E = 0.7$ meV. (B) Wave vector and energy dependence of the exciton-polariton radiative lifetime (calculated). The color scale is in units of picoseconds (red color represents longer lifetime). (C) (Top and Middle) Real and imaginary parts of the complex potential induced by the Si grating for the microrod polaritons. The “air” and “silicon” represent, respectively, the freestanding parts and silicon-contacting parts of the microcavity. (Bottom) Sketch of the probability amplitude distribution ($|\Psi|^2$) for the states labeled as A and A' in Fig. 3B. (D) Spatially resolved PL image obtained by exciting the microrod step-by-step along the z axis. The full width at half maximum of the pulsed excitation laser is about $1 \mu\text{m}$. The emission bright regions are pinned to the period potential. (E–G) Spatial coherence analysis from a Michelson interferometer. (E and F) Real-space PL mappings measured by each arm of the interferometer. (F) The second arm with a retroreflector flips the image E. The excitation source in this experiment was a pulsed laser (wavelength: 355 nm, diameter of the laser spot: $10 \mu\text{m}$). (G) The coherent overlapping between the two images of the condensates forms the interference pattern. The interference fringes appear because of a small inclination angle between the images from the two arms of the interferometer.

which is substantially smaller than the theoretically expected saturation value 1.5 for an ideal 1D lattice. This discrepancy is presumably due to the strong disorder present in the ZnO microrod, which is clearly seen from fluctuations in the amplitudes of the peaks in Fig. 4D.

Previous low-temperature experiments on GaAs-based polariton superlattices (17) evidenced polariton lasing from the edge of the Brillouin zone but no period doubling. We believe that the weak lasing phase in ZnO polariton superlattices is robust because both real and imaginary parts of the periodic potential are modulated much stronger than in the planar GaAs microcavity with a metallic pattern on the top studied in ref. 17.

In conclusion, by the nonresonant optical pumping of a ZnO microrod-Si grid superlattice we created a condensate of exciton-polaritons at room temperature and proved its long-range phase coherence. At sufficiently strong pumping the spatial pe-

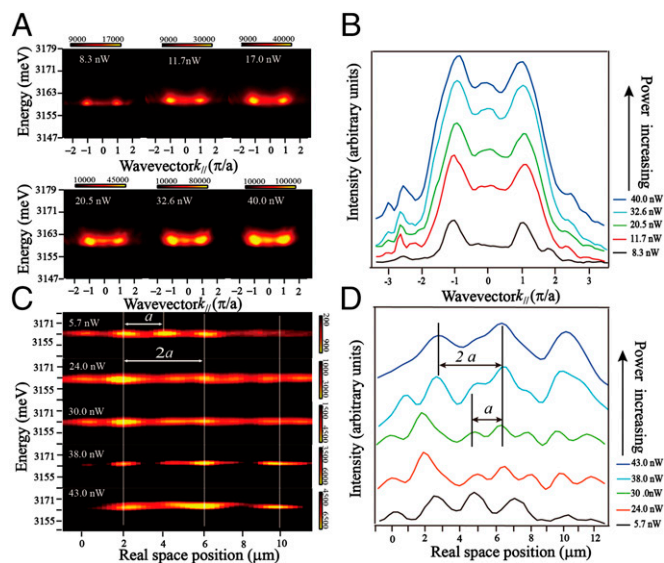


Fig. 4. Phase transition from π -state condensation to weak lasing. (A) The evolution of polariton condensates in momentum space with increasing pump power. The experiments were carried out on another sample. (B) The power dependence of the PL intensity at the lasing frequency in k space. At the threshold of about 20 nW, a small peak appears at $k_{\parallel} = 0$. Its frequency corresponds to the edges of the Brillouin zone. (C) The evolution of the polariton condensate's distribution in real space with increasing excitation power. (D) The power dependence of the PL intensity at the lasing frequency in real space. At the threshold of 20 nW, the period of the polariton condensate is doubled compared with the period of the superlattice.

riod of the condensate turned out to be twice as long as the period of the superlattice. This spontaneous symmetry breaking strongly suggests that the weak lasing regime of polariton condensation has been achieved in our experiments.

Materials and Methods

The experimental setup is detailed in ref. 16. The ZnO microwires used here were synthesized by a chemical vapor deposition method. Instead of directly depositing a periodic pattern on the top surface of a microcavity, which might induce intrinsic structural diffraction, we laid the ZnO microrod on a silicon slice with periodically arranged channels. They contacted closely due to the van der Waals force. This microassembled structure introduced an additional modulation to the ZnO polariton energies and lifetimes in the z direction (crystallographic c direction). The resonance energies of the cavity are shifted due to the variation of the effective refractive index induced by the silicon substrate, which results in the appearance of a superlattice potential. To characterize the polariton states in this structure we detected the photoluminescence signal from the top surface of the microcavity.

ACKNOWLEDGMENTS. We thank Jacqueline Bloch, Eugenius Ivchenko, and Igor Aleiner for many stimulating discussions. We thank David Snok for critical reading of the manuscript and helpful remarks. The work is funded by the 973 projects of China (2011CB925600), National Science Foundation of China (91121007, 11225419, and 11304042), and the European Union FP7 Marie Curie Actions-International Research Staff Exchange Scheme Project “Polarization phenomena in Semiconductor Microcavities”. A.P. acknowledges the support of the “Dynasty” foundation and Russian President Grant MK-6029.2014.2. A.V.K. acknowledges the support from the Russian Ministry of Education and Science (Contract 11.G34.31.0067).

- Esaki L, Chang LL (1974) New transport phenomenon in a semiconductor “superlattice.” *Phys Rev Lett* 33(8):495–498.
- Robertson WM, et al. (1992) Measurement of photonic band structure in a two-dimensional periodic dielectric array. *Phys Rev Lett* 68(13):2023–2026.
- Colvard C, Merlin R, Klein MV, Gossard AC (1980) Observation of folded acoustic phonons in a semiconductor superlattice. *Phys Rev Lett* 45(4):298–301.

- Brückner R, et al. (2012) Phase-locked coherent modes in a patterned metal-organic microcavity. *Nat Photonics* 6(5):322–326.
- Hopfield JJ (1958) Theory of the contribution of excitons to the complex dielectric constant of crystals. *Phys Rev* 112(5):1555–1567.
- Deng H, Weihs G, Santori C, Bloch J, Yamamoto Y (2002) Condensation of semiconductor microcavity exciton polaritons. *Science* 298(5591):199–202.

7. Weisbuch C, Nishioka M, Ishikawa A, Arakawa Y (1992) Observation of the coupled exciton-photon mode splitting in a semiconductor quantum microcavity. *Phys Rev Lett* 69(23):3314–3317.
8. Amo A, et al. (2009) Collective fluid dynamics of a polariton condensate in a semiconductor microcavity. *Nature* 457(7227):291–295.
9. Wertz E, et al. (2010) Spontaneous formation and optical manipulation of extended polariton condensates. *Nat Phys* 6(11):860–864.
10. Sich M, et al. (2012) Observation of bright polariton solitons in a semiconductor microcavity. *Nat Photonics* 6(1):50–55.
11. Sanvitto D, et al. (2010) Persistent currents and quantized vortices in a polariton superfluid. *Nat Phys* 6(7):527–533.
12. Wouters M, Carusotto I (2007) Excitations in a nonequilibrium Bose-Einstein condensate of exciton polaritons. *Phys Rev Lett* 99(14):140402.
13. Carusotto I, Ciuti C (2013) Quantum fluids of light. *Rev Mod Phys* 85(1):299–366.
14. Aleiner IL, Altshuler BL, Rubo YG (2012) Radiative coupling and weak lasing of exciton-polariton condensates. *Phys Rev B* 85(12):121301(R).
15. Sun L, et al. (2008) Direct observation of whispering gallery mode polaritons and their dispersion in a ZnO tapered microcavity. *Phys Rev Lett* 100(15):156403.
16. Xie W, et al. (2012) Room-temperature polariton parametric scattering driven by a one-dimensional polariton condensate. *Phys Rev Lett* 108(16):166401.
17. Lai CW, et al. (2007) Coherent zero-state and pi-state in an exciton-polariton condensate array. *Nature* 450(7169):529–532.
18. Borrmann G (1950) Die Absorption von Röntgenstrahlen im Fall der Interferenz. *Z Phys* 127:297–323.
19. Poddubny AN, Rybin MV, Limonov MF, Kivshar YS (2012) Fano interference governs wave transport in disordered systems. *Nat Commun* 3:914–924.